Journal of Photopolymer Science and Technology
Volume 28, Number 2 (2015) 255–260 © 2015SPST

Luminescent Silicon Nanoparticles Surface-Modified with Chiral Molecules

Mari Miyano[1], Takayuki Nakanishi[1]*, Satoshi Wada[1], Yuichi Kitagawa[1], Akira Kawashima[1], Koji Fushimi[1], Yasuhiro Morisaki[2,3], Yoshiki Chujo[3] and Yasuchika Hasegawa[1]*

[1]Faculty of Engineering, Hokkaido University, N13 W8, Kita-ku, Sapporo, Hokkaido 060-8628, Japan,
[2]School of Science and Technology, Kwansei Gakuin University, 2-1, Gakuen, Mita-shi, Hyogo 669-1337, Japan (Present address)
[3]Graduate School of Engineering, Kyoto University, Nishikyo-ku, Kyoto 615-8510, Japan
**hasegaway@eng.hokudai.ac.jp (Y. Hasegawa)*

Active surface of luminescent silicon nanoparticles was terminated by the photochemical reaction of chiral molecules, (*S*)- or (*R*)-5-allyl-2-oxabicyclo[3,3,0]oct-8-ene ((*S*) - or (*R*) - AOBE) under UV light. The particle size and shapes were characterized using Transmission Electron Microscope (TEM). The average particle size was found to be 5.7 nm. Circular dichroism (CD) signals with large dissymmetry factors from silicon nanoparticles terminated with (*S*) - and (*R*) - AOBE were observed at around 300 nm and 500 nm, which were much larger than those of (*S*)- and (*R*)-AOBE molecules. The silicon nanoparticles covered with (*S*)- or (*R*)-AOBE provided red luminescence based on the indirect electronic transition. Effective circular polarized luminescence (CPL) was not observed from indirect transition band.

Keywords: quantum dot, silicon, chiral molecules, surface protection, circular dichroism

1. Introduction

Luminescent silicon nanoparticles have gained considerable attention for their potential applications such as light-emitting diodes, lasers, solar cells, and bio-sensing applications [1-13]. The luminescence of silicon nanoparticles is based on their indirect electronic transition, which comes from the direct re-combination of excited electrons and positive holes based on the wave function overlap in the nanometer range, quantum confinement effect [14]. The energy gap of silicon nanoparticles can also be manipulated by control of the particle size, due to the quantum size effect. Quantum-sized silicon nanoparticles have been focused as a considerable luminescent semiconductor material with a tunable quasi-direct transition band.

Recently, surface-modifications on the silicon nanoparticle have been studied for control of their photo physical properties. In particular, surface protection using organic molecules on the silicon nanoparticles leads to enhancement of luminescence quantum yield. Swihart and coworkers have described luminescent silicon nanoparticles covered with polystyrene [15]. We prepared luminescent silicon nanoparticles using photochemical reaction of styrene molecules with Si-H bond on the surface [16]. Recently, surface protection using ionic liquid for prevention of oxidation of silicon nanoparticles has been described [17]. At the present stage, various types of surface protection studies on the silicon nanoparticles have been reported [18-19].

The surface protection of silicon nanoparticles is useful for development of novel luminescent and photo-functional nanomaterials. Here, we focus on the surface protection using organic chiral molecules for photo-functional nanomaterials. Generally, metal complex with chiral molecules provides asymmetric coordination structure. The asymmetric structures promote effective chiroptical signals on the circular dichroism (CD) and circularly polarized luminescence

Received April 15, 2015
Accepted May 25, 2015

(CPL) spectra. In particular, lanthanide complexes with chiral molecules show large CPL signals, which are expected to be useful in future chiroptical applications such as three dimensional display and chiroptical memory [20]. Chiroptical memory and sensor using CdTe, and CdSe/ZnO nanoparticles rapped with chiral molecules have been suggested [21-22]. Recently, induced CD and CPL properties in CdSe quantum dots have been reported [23]. There chiroptical properties of metal complexes and semiconductor nanoparticles are based on direct electronic transition of energy gaps.

In this study, we have attempted to observe the indirect electronic transition of silicon nanoparticle attached with chiral molecules. The chiral molecules, (*S*)- and (*R*)-5-allyl-2-oxabicyclo[3,3,0]oct-8-ene ((*S*) - AOBE and (*R*) - AOBE) are shown in Fig. 1. The silicon nanoparticles with (*S*) - or (*R*) - AOBE were characterized using Transmission Electron Microscope (TEM). The chiroptical properties were observed using CD spectra. CD signals with large dissymmetry factors from silicon nanoparticles terminated with (*S*) - and (*R*) - AOBE were observed at around 300 nm and 500 nm, which were much larger than those of (*S*) - and (*R*) - AOBE molecules. Indirect CPL properties of chiral molecules terminated silicon are also discussed. Optical properties of chiral molecules-terminated silicon nanoparticles are demonstrated for the first time.

The reaction mechanism of the diazonaphtho-quinonenovolac resist on light-exposure has been explained in text books [1] as represented in Fig. l(a): i.e. , the base-insoluble photochemically active compound (PAC), a diazonaphthoquinone, undergoes photolysis to produce a carbene which then undergoes Wolff rearrangement to form a ketene. The ketene adds water, which is present in the resist fiom, to form a base-soluble indencarboxylic acid, the final product [2]. This mechanism is very similar to that of the bisarylazide-rubber resist shown in Fig.1(b) in its primary photo-event[3]; i.e. , the bisazide undergoes photolysis to produce a nitrene which forms a linkage between two polymer chains of rubber. However, these two kinds of photoresist is insensitive to atomospheric oxygen.

2. Method

2.1 Materials

Tetra-ethoxysilane ES40 as a source for silicon was purchased from COLCOAT CO.LTD. Phenol resin SR-101 as a source of carbon was obtained from AIR

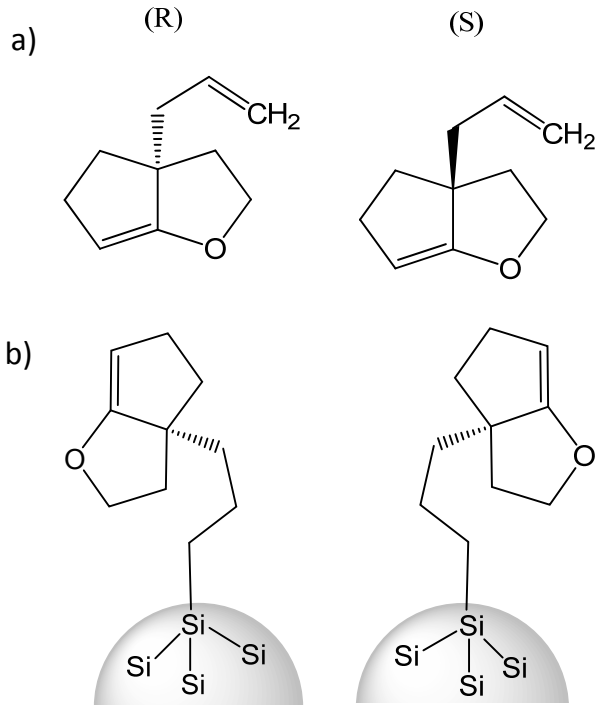

Fig. 1 (a) Structures of (*R*)-5-Allyl-2-oxabicyclo[3,3,0] oct-8-ene ((*R*) - AOBE) and (*S*)-5-Allyl-2-oxabicyclo [3,3,0]oct-8-ene ((*S*) - AOBE). (b) Image structure of (*R*) - or (*S*) - AOBE terminated on silicon nanoparticle.

WATER INC. Aqueous solution of maleic acid (70 %) as a catalyst was purchased from Nippon Syokubai. Hydrofluoric acid HF (48 %) was purchased from Wako Pure Chemical Industries, Ltd.. Nitric acid HNO_3 (62%) and styrene were purchased from Kanto Chemical Co., Inc.. Trichloromethane (Chloroform) was purchased from Wako Pure Chemical Industries, Ltd.. (*R*)-5-Allyl-2-oxabicyclo[3,3,0]oct-8-ene ((*R*) - AOBE) and (*S*)-5-allyl-2-oxabicyclo[3,3,0]oct-8-ene ((*S*) - AOBE) were purchased from Sigma-Aldrich. Polyethylene filter was obtained by Japan Entegris Inc.

All other chemicals and solvents were reagent grade and were used without further purification.

2.2 Apparatus

UV light source (wavelength at 365nm) was used a LED365-SPT/L (Optocode Corp) for observation of acid-etching process. Their emission spectra under acid-etching process were measured using Hamamatsu Photonics Co. Ltd., PMA-12 photonic multichannel analyzer. UV cross-linker, as a photo-assisted reactor (Funakoshi Co.) is used for the photo-chemical reaction of (*S*)- or (*R*) - AOBE with silicon surface. Silicon

nanoparticles covered with (*S*) - or (*R*) - AOBE were obtained with a TEM, JEOL 2010 FASTEM (200 kV).

2.2.1 Acid-etching process of silicon nanoparticles for control of particle size

Silicon nanoparticles were obtained using the same method as previous reported [16]. The silicon nanoparticles (4 mg) and methanol (4 ml) were placed into a polypropylene container with the simultaneous addition of 10 mL of 48% HF and 2 mL of 68% nitric acid (HNO_3). Acid etching of the silicon nanoparticle was performed under ultrasonication at 20 °C. The acid etching process was monitored by observation of the silicon nanoparticle luminescence under excitation with UV light (365 nm). The acid-etching process was stopped by the addition of methanol solution (water: methanol = 3:1 v/v, 30 ml) to the solution. After the acid etching process, the solution was filtered using a polyethylene filter (20 nm mesh) and the residue (silicon nanoparticles) was washed with 5 mL of 2% HF to eliminate the thin surface oxidation layer, followed by rinsing twice with 5 mL of purified water to completely wash off the acid. The material obtained was vacuum-dried at room temperature for 60 min to completely remove water.

2.2.2 Surface Protection Process

The acid-etched silicon nanoparticles were placed into 1.5 mL of (*S*)- or (*R*) - AOBE. The dispersion of silicon nanoparticles in (*S*) - or (*R*) - AOBE were agitated using a magnetic stirrer under irradiation with UV light (λ = 365 nm) for hydrosilylation on the surface of the silicon nanoparticles. The resultant solution was centrifuged (7000G) for 60 min at 15 °C to eliminate by-products such as SiC and aggregates of silicon nanoparticles, which resulted in the formation of mono dispersed silicon nanoparticles bonded with (*S*)- or (*R*)-AOBE.

2.2.3 Optical measurements

Emission spectra from surface-terminated silicon nanoparticles in termination reagent were measured by using a Hitachi High Technologies Co. F-7000**.** The emission quantum yield of surface-terminated silicone nanoparticles were measured using a Hamamatsu Photonics Co. Ltd. C9920-02G system. CD spectra were measured using JASCO J-1500 spectropolarimeter. CPL spectra were measured using JASCO CPL-200 spectrofluoropolarimeter (excitation wavelength = 380 nm).

3. Results

3.1 Characterization

Silicon nanoparticles attached with (*S*) - or (*R*) - AOBE under UV irradiation was prepared using photochemical reaction. The photochemical reaction induces the formation of Si-C bond from vinyl group of the molecules on the silicon surface (Fig. 1). We have reported the formation of the Si-C bond between styrene molecule with vinyl group and silicon, previously. The formation of Si-C bonds on the silicon surface leads to enhancement of the emission quantum yield [16]. Silicon nanoparticles with (*S*) - or (*R*) - AOBE also show effective red luminescence. In contrast, silicon nanoparticles without surface protection do not emit photon [17]. We consider that surface of silicon nanoparticles may be directly linked to (*S*) - or (*R*) - AOBE molecules.

The TEM image and the size distribution of silicon nanoparticles with (*R*) - AOBE are shown in Fig. 2. We observed mono dispersion histogram of silicon nanoparticles on the TEM image. The average size of silicon nanoparticles was estimated to be 5.7 nm (200 counts). This size distribution and average size of silicon nanoparticles with (*R*)-AOBE is similar to those of silicon nanoparticles with styrene molecules (5.0 nm). Previously, we have reported the quantum size effect on the wavelength of the emission of silicon nanoparticles [16]. The wavelength of the emission for silicon nanoparticles with styrene molecules (average size = 5.0 nm) was found to be 750 nm. Based on the previous study, the emission of silicon nanoparticles with (*R*) - AOBE might be observed at around 750 nm.

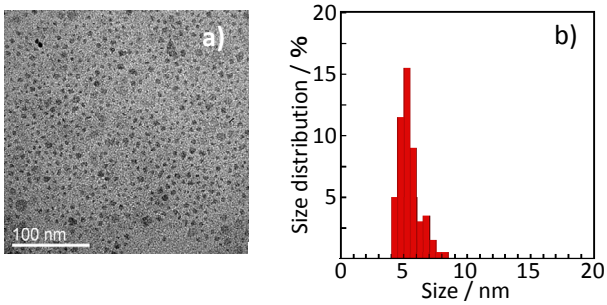

Fig. 2 (a) TEM image of (*R*) - AOBE terminated silicon nanoparticles. (b) Size distribution of (*R*) - AOBE terminated silicon nanoparticles.

3.2 CD spectra of Silicon Nanoparticles with Chiral Molecules

The electronic absorption spectra of (*R/S*) - AOBE and silicon nanoparticles with (*R/S*) AOBE (Si - (*R/S*) -AOBE) are shown in Fig. 3(a)-(1-4). The intense absorption bands due to the π-π* transition are observed around 240 nm for (*R/S*) - AOBE (Fig. 3(a)-(1-2)). The bands are broadened and scarcely shift to the red-side by the modifications on the surfaces of the Si - (*R/S*) - AOBE, (Fig. 3(a)-(3-4)). The results indicate the formation of the new electronic states due to the covalent bonds with the surface silicon atoms. The several shoulder peaks were also observed for Si - (*R/S*) - AOBE, which originate from the interband transitions of the silicon nanoparticle [19].

The CD spectra of (*R/S*) - AOBE and Si - (*R/S*) - AOBE are shown in Fig. 3(b)-(1-4). The CD signals of the π-π* transitions are observed around 240 nm for (*R/S*) - AOBE (Fig. 3(b)-(1-2)). According to the Si-(*R/S*) - AOBE, the CD signals are observed at not only the π-π* transitions, but the interband transitions of the silicon nanoparticles (Fig. 3(b)-(3-4)). The results indicate that the mixing of electronic states of (*R/S*) - AOBE with those of surface silicon atoms induces the chirality of the silicon nanoparticles. These CD intensities are estimated by the dissymmetry factor, g_{CD}. In general, g_{CD} is gained by the following equation,

$$g_{CD} = 4\frac{|m|}{|\mu|}\cos\theta \quad (1)$$

The g_{CD} of the interband transitions of Si - (*R/S*) - AOBE at around 300 nm (Si - (*R*) -AOBE: $g_{(300\ nm)} = 4.7\times10^{-3}$, Si - (*S*) -AOBE: $g_{(300\ nm)} = 8.7\times10^{-3}$) and 500 nm (Si - (*R*) -AOBE: $g_{(516\ nm)} = 2.3\times10^{-2}$, Si - (*S*) -AOBE: $g_{(511\ nm)} = 1.2\times10^{-2}$) are much larger than those of (*R/S*) – AOBE ((*R*) – AOBE: $g_{max(250nm)} = 1.7\times10^{-3}$, (*S*) – AOBE: $g_{max(250nm)} = 1.6\times10^{-3}$). Thus, we successfully synthesized the silicon nanoparticle exhibiting large chiropical properties for the first time by the surface modification with the chiral organic compounds. The induced CD signals on semiconductor such as CdSe nanoparticles

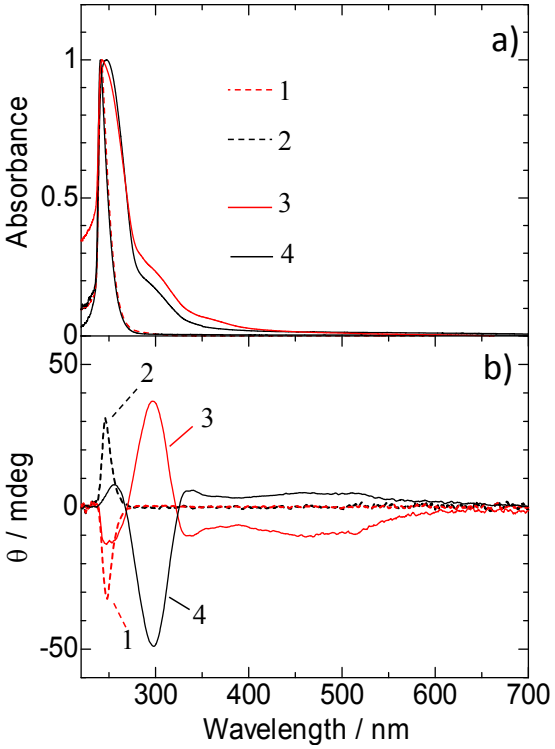

Fig. 3 (a) Absorption spectra of (*R*) - AOBE (1), (*S*) - AOBE (2) Si - (*R*) - AOBE (3) and Si - (*S*) - AOBE (3) in trichloromethane. (b) CD spectra of (*R*) - AOBE (1), (S) - AOBE (1) Si - (*R*) - AOBE (1) and Si - (*S*) - AOBE (4) in trichloromethane.

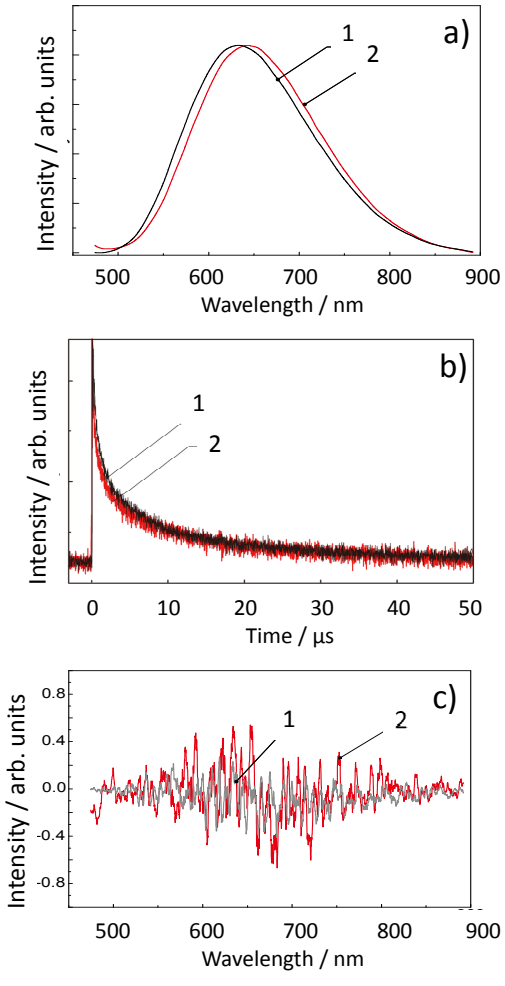

Fig. 4 (a) Emission spectra of Si - (*R*) - AOBE (1) and Si - (*S*) - AOBE (2) in trichloromethane. (b) Emission decay profiles of Si - (*R*) - AOBE (1) and Si - (*S*) - AOBE (2) in trichloromethane. (c) CPL spectra of Si - (*R*) - AOBE (1) and Si - (*S*) - AOBE (2) in trichloromethane.

have been observed, previously [22]. We proposed that the induced CD signals on Si - (*R/S*) - AOBE may be caused by the electronic interaction between π-π*orbitals of (*R/S*) - AOBE and silicon surface.

3.3 Emission properties of Silicon Nanoparticles with Chiral Molecules

The emission spectra of Si - (*R/S*) - AOBE excited at 250nm are shown in Fig. 4(a). We observed effective red luminescence at around 630 nm. The emission wavelength from Si - (*S*) - AOBE is much similar to that of Si - (*R*) - AOBE. The slight blue shift of the emission from Si - (*R*) - AOBE (< 2 nm) might be due to percentage of modified AOBE on the silicon surface. The time-resolved emission decay profiles of the Si -(*R/S*) - AOBE are also shown in Fig. 4(b). The emission profiles revealed mluti-exponetial decay with lifetimes in the microsecond timescales. The emission decay of Si - (*R*) - AOBE is much similar to that of Si - (*S*) - AOBE.

The emission wavelengths of previous reported silicon nanoparticles with styrene molecules (average size = 5.0 nm) are longer than that of corresponding Si - (*R/S*) - AOBE (average size = 5.7 nm). The red shift of previous silicon with styrene might be due to specific interaction between silicon surface and aromatic ring of the styrene units [21]. We have reported that the emission quantum yield of silicon nanoparticles with styrene molecules (emission wavelength = 680 nm) was found to be 55 %. The emission quantum yield of Si - (*R/S*) - AOBE should be approximately 50 %.

In order to estimate the chiroptical properties on the emission of silicon nanoparticles, we carried out CPL spectral measurements of Si - (*R/S*) - AOBE. The CPL spectra are shown in Fig. 4c. Characteristic CPL signals at around emission area were not observed (spectra show noisy signals). The emission of silicon nanoparticles comes from "indirect transition" in the conduction band in silicon semiconductor. On the other hand, effective CPL signals of "direct transition" in CdSe nanoparticles have been reported, previously [23]. We propose that asymmetric structural information using chiroptical molecules on the silicon surface affects on absorption band as an induced CD signals, however, does not affect on the "indirect transition" of the emission process.

4. Conclusion

We successfully prepared silicon nanoparticles with chiroptical molecules, Si - (*R/S*) - AOBE. The dissymmetry factor g_{CD} on CD spectra of Si - (*R/S*) - AOBE are much larger than that of (*R/S*) - AOBE molecules. The silicon surface affects on the CD signals of (*R/S*) - AOBE. This is the first observation of enhanced chroptical properties of silicon nanoparticles. The signal intensity and active-area of chiral molecules are dominated on the silicon nanoparticle surface. The photophysical aspects would be useful in application such as future chroptical sensors and devices.

Acknowledgments

This work was party supported by Grants-in-Aid for Scientific Research on Innovative Areas of New Polymeric Materials Based on Element-Blocks (No. 2401) (24102012) of the Ministry of Education, Culture, Sports, Science and Technology (MEXT) of Japan.

References

1. J. A. Kelly, J. G. C. Veinot, *ACS Nano*, **4** (2010) 4645.
2. R. J. Clark, M. K. M. Dang, J. G. C. Veinot, *Langmuir*, **26** (2010) 15657.
3. F. Hua, M. T. Swihart, E. Ruckenstein, *Langmuir*, **21** (2005) 6054.
4. S. Takeoka, M. Fujii, S. Hayashi, *Phys. Rev. B*, **62** (2000) 16820.
5. C. Linyou, F. Pengyu, S. E. Barnard, M. A. Brown, L. M. Brongersma, *Nano Lett.*, **10** (2010) 2649.
6. J. M. Llansola Portolés, P. R. Dies, L. M. Dell'Arciprete, P. Caregnato, J. J. Romero, O. D. Mártire, O. Azzaroni, M. Ceolin, C. M. Gonzalez, *J. Phys. Chem. C*, **116** (2012) 11315.
7. Z. Yang, A. R. Dobbie, K. Cui, J. G. C. Veniot, *J. Am. Chem. Soc.*, **134** (2012) 13958.
8. L. M. Mastronardi, F. Hennrich, J. E. Henderson, F. Maier-Flaig, C. Blum, J. Reichenbach, U. Lemmer, C. Kübel, D. Wang, M. M. Kappes, A. G. Ozin, *J. Am. Chem. Soc*., **133** (2011) 11928.
9. Q. Li, Y. He, J. Chang, L. Wang, H. Chen, Y.-W. Tan, H. Wang, Z. Shao, *J. Am. Chem. Soc.,* **135** (2013) 14924.
10. A. Shiohara, S. Hanada, S. Prabakar, K. Fujioka, T. H. Lim, K. Yamamoto, P. T. Northcote, D. R. Tilley, *J. Am. Chem. Soc.*, **132** (2010) 248.
11. B. A. Manhat, A. L. Brown, L. A. Black, J. B. A. Ross, K. Fichter, T. Vu, E. Richman, A. M. Goforth, *Chem. Mater*., **23** (2011) 2407.
12. S. Sato, M. T. Swihart, *Chem. Mater.*, **18** (2006) 4083.
13. H. Ohno, A. Shen, F. Matsukura, A. Oiwa, A. Endo, S. Katsumoto, Y. Iye, *Appl. Phys. Lett.*, **69** (1996) 363.

14. N. Koshida, N. Matsumoto, *Mater. Sci. Eng.*, *R*, **40** (2003) 169.
15. X. Li, Y. He, S. S. Talukdar, M. T. Swihart, *Langmuir*, **19** (2003) 8490.
16. M. Miyano, S. Endo, H. Takenouchi, S. Nakamura, Y. Iwabuti, O. Shiino, T. Nakanishi, Y. Hasegawa, *J. Phys. Chem. C*, **118** (2014) 19778.
17. M. Miyano, S. Wada, T. Nakanishi, Y. Hasegawa, *Mater. Lett.*, **141** (2015) 359.
18. M. Dasog, G. B. De los Reyes, L. V. Titova, F. A. Hegmann, J. G. C. Veinot, *ACS Nano*, **8** (2014) 9636.
19. J. J. Romeo, M. J. Llansola-Portolés, M. L. Dell' Arciprete, H. B. Rodriguez, A. L. Moore, M. C. Gonzalez, *Chem. Mater.*, **25** (2013) 3488.
20. T. Harada, Y. Nakano, M. Fujiki, M. Naito, T. Kawai, Y. Hasegawa, *Inorg. Chem.*, **48** (2009) 11242.
21. T. Nakashima, Y. Kobayashi, T. Kawai, *J. Am. Chem. Soc.*, **131** (2009) 10342.
22. T. Delgado-Pérez, L. M. Bouchet, M. de la Guardia, R. E. Galian, J. Pérez-Prieto, *Chem. Eur. J.*, **19** (2013) 11068.
23. U. Tohgha, K. K. Deol, A. G. Porter, S. G. Bartko, J. K. Choi, B. M. Leonard, K. Varga, J. Kubelka, G. Muller, M. Balaz, *ACS Nano*, **7** (2013) 11094.